Date of publication xxxx 00, 0000, date of current version xxxx 00, 0000.

Digital Object Identifier 10.1109/ACCESS.2017.DOI

Electromagnetic inverse scattering of rotating axisymmetric objects

PRAVEEN KALARICKEL RAMAKRISHNAN, MARIO RENE CLEMENTE VARGAS, AND MIRCO RAFFETTO

Department of Electrical, Electronic, Telecommunications Engineering and Naval Architecture, University of Genoa, Genoa, Italy

Corresponding author: Praveen Kalarickel Ramakrishnan (e-mail: pravin.nitc@gmail.com).

ABSTRACT The electromagnetic inverse scattering problem for rotating axisymmetric objects is studied. A modification of a previously proposed two-step algorithm is adopted to obtain the first solutions of the problems of interest. In the first step, the forward solver is employed assuming zero rotating speed and the geometric and dielectric parameters are reconstructed by minimizing the cost function. In the second step, the values from the first step are used to determine the rotating speed. Numerical results for this type of inverse problems are provided for the first time by considering test cases with rotating homogeneous sphere and torus. The two-step algorithm is compared against the general inversion algorithm that relies on global optimization considering all unknown variables simultaneously. It is demonstrated that the proposed algorithm outperforms the general inversion procedure for all speeds of practical interest. The results are analyzed for noisy data in the near-field and far-field.

INDEX TERMS Electromagnetic scattering, inverse problems, moving media, stochastic optimization, remote sensing, rotating axisymmetric objects.

I. INTRODUCTION

The electromagnetic problems involving moving objects are important in numerous applications like astrophysics, nuclear physics, plasma physics and engineering [1], [2], [3], [4], [5]. Although the most general problems need to be formulated in time domain [2], there are important applications where the motion of the objects is such that a frequency domain formulation is feasible [6]. The moving media behave as bianisotropic materials in the laboratory frame even when they are isotropic in the rest frame [7].

A very important class of the problems involves rotating axisymmetric objects which can be studied using three-dimensional time-harmonic models [1], [8]. A set of sufficient conditions for well posedness and the finite element approximability of the forward problem of calculating the fields were established in [8]. In some of the indicated problems the rotating velocity is not known and it is of particular interest to be able to detect it using inverse scattering procedures. However, to the best of authors' knowledge, there are no results on the detection of the rotating velocity from scattered field data.

In [9] the authors developed a two-step algorithm for the reconstruction of the velocity of two-dimensional problems involving axially moving cylinders when the speeds are not too large. The idea was based on the fact that for a particular polarization of incident field (TM or TE), one of the polarizations (cross-polarized component) is absent in the scattered field when there is no motion and varies linearly with the velocity for small speeds. In addition, the other polarization of the scattered field (co-polarized component) is affected only slightly (second order effect) due to motion. This led to the algorithm in which the co-polarized component of the scattered field is used in the first step to reconstruct the dielectric and geometric properties of the media by ignoring the effects of motion. The values deduced with the first step where then used in the second step to find the axial speed from the cross- polarized component. The authors were able to demonstrate the efficiency of the two-step procedure over directly using the whole field in a single step to simultaneously reconstruct all the unknowns. The better performance of the two-step procedure stems from the fact that the complexity of the inversion algorithm increases much faster than linear with the number of unknowns and hence the solution using two simpler steps is much more efficient than solving the full problem in one large step. Further, in [10], the authors studied the limitations of the reconstruction algorithm when the measured data are noisy and the sensors have limited capabilities.

In general three-dimensional problems the effects of bian-

isotropy are more complex [8], [11] and it could be difficult or even impossible to isolate field components able to provide so clear indication on the velocity field. The first numerical results for the fields in the presence of motion were presented in [8] and they indicate that the effect due to motion is not too large even for relatively high values of rotating speeds. Therefore, in this case, we propose to define a cost function using all the components of the fields in the first step which is used to reconstruct the geometric and dielectric properties assuming that the media is under rest. In the second step the values from the first step are used to evaluate the speed of rotation. For small rotating speed, the numerical results demonstrate that such an approach is effective and fast compared to inverting all the unknowns in a single step. The numerical results are obtained for a test problem involving a homogeneous rotating sphere which admits an analytic solution [1]. The robustness of the results are demonstrated by examining the effect of different levels of noise in the input data. The results are demonstrated also for different measurement scenarios with amplitude and phase data from near-field or from far-field. The effect of using simple sensors with only amplitude data is also studied. Within the range of rotating speeds considered, the reconstruction can obtain accurate values even for large noise levels if the speed is large enough. In case of small rotating speeds, the inversion can give correct values if the noise levels can be reduced to lower levels. Finally, to show the generality of the approach, results are provided for a test case involving rotating torus. For this case, the forward solver employed uses the finite element method in the absence of an analytic solver.

The article is organized as follows. In Section II the problem is defined and the two-step algorithm employed for the inversion procedure is explained in detail. In Section III the numerical results for the inversion process are provided and the efficiency and reliability of the two-step procedure are studied. Finally, the conclusions of the article are discussed in Section IV.

II. INVERSION PROCEDURE FOR ROTATING MEDIA

As mentioned in the previous section, the reconstruction of velocity profiles of moving media using electromagnetic inverse scattering techniques is an important subject. Such techniques have been exploited for axially moving cylinders in [9], [10]. Here we study the reconstruction of the rotating speeds of axisymmetric media, which has numerous practical applications, for example in the tachometry of celestial bodies [2], [1], [8].

The unknown parameters of the inverse scattering problem may be represented by the algebraic vector $\mathbf{u} = (\mathbf{u}_g, \mathbf{u}_d, \mathbf{u}_v) \in \mathbb{R}^{I+J+K}$, where $\mathbf{u}_g \in \mathbb{R}^I$, $\mathbf{u}_d \in \mathbb{R}^J$ and $\mathbf{u}_v \in \mathbb{R}^K$ are respectively the components having the geometric, dielectric and velocity parameters [9].

A set of S plane wave sources illuminate the scatterer. The positions of the sources are denoted by an integer parameter $s = 1, ..., S$. The electric and magnetic fields are measured using M sensors whose positions are indicated by the parameter $m = 1, ..., M$. The measured electric and magnetic fields are denoted respectively by $\mathbf{E}^{meas}(s, m, \mathbf{u})$ and $\mathbf{H}^{meas}(s, m, \mathbf{u})$.

For a trial solution $\mathbf{u}^{trial} = (\mathbf{u}_g^{trial}, \mathbf{u}_d^{trial}, \mathbf{u}_v^{trial}) \in \mathbb{R}^{I+J+K}$, we may assume to have a forward scattering procedure (fsp), either semi analytic [1] or numerical [8], that enables us to calculate the fields $\mathbf{E}^{fsp}(s, m, \mathbf{u}^{trial})$ and $\mathbf{H}^{fsp}(s, m, \mathbf{u}^{trial})$.

The above quantities can be used to define the following cost function, which is to be minimized using an optimization algorithm to get the best estimate of the unknown parameters:

$$CF(\mathbf{u}, \mathbf{u}^{trial}) = \frac{\sum_{s=1}^{S}\sum_{m=1}^{M} ||\mathbf{E}^{fsp}(s, m, \mathbf{u}^{trial}) - \mathbf{E}^{meas}(s, m, \mathbf{u})||^2}{\sum_{s=1}^{S}\sum_{m=1}^{M} ||\mathbf{E}^{meas}(s, m, \mathbf{u})||^2} + \frac{\sum_{s=1}^{S}\sum_{m=1}^{M} ||\mathbf{H}^{fsp}(s, m, \mathbf{u}^{trial}) - \mathbf{H}^{meas}(s, m, \mathbf{u})||^2}{\sum_{s=1}^{S}\sum_{m=1}^{M} ||\mathbf{H}^{meas}(s, m, \mathbf{u})||^2}. \quad (1)$$

Here the norms are just Euclidean norms for three-dimensional complex vectors.

The above steps provide the general way to obtain the parameters using the inverse scattering algorithm. However, if the velocity of the rotating objects are small enough, then we may adopt a two-step procedure for the inversion. Since the contribution to the fields due to the rotation will be small, the media may be assumed to be at rest for the reconstruction of geometric and dielectric data. Thus the cost function for the first step will be as follows:

$$CF_1(\mathbf{u}, \mathbf{u}_1^{trial}) = \frac{\sum_{s=1}^{S}\sum_{m=1}^{M} ||\mathbf{E}^{fsp,rest}(s, m, \mathbf{u}_1^{trial}) - \mathbf{E}^{meas}(s, m, \mathbf{u})||^2}{\sum_{s=1}^{S}\sum_{m=1}^{M} ||\mathbf{E}^{meas}(s, m, \mathbf{u})||^2} + \frac{\sum_{s=1}^{S}\sum_{m=1}^{M} ||\mathbf{H}^{fsp,rest}(s, m, \mathbf{u}_1^{trial}) - \mathbf{H}^{meas}(s, m, \mathbf{u})||^2}{\sum_{s=1}^{S}\sum_{m=1}^{M} ||\mathbf{H}^{meas}(s, m, \mathbf{u})||^2}. \quad (2)$$

Here the vector $\mathbf{u}_1^{trial} = (\mathbf{u}_g^{trial}, \mathbf{u}_d^{trial})$ contains the geometric and dielectric unknowns and the fields are calculated with the analytic or numerical solver for the rest case.

In the second step, we estimate the velocity by optimizing the following cost function that uses forward scattering procedure for the rotating media along with the approximate geometric and dielectric data $\mathbf{u}_1^{as}$ obtained from the previous step:

$$CF_2(\mathbf{u}, \mathbf{u}_1^{as}, \mathbf{u}_v^{trial}) = \frac{\sum_{s=1}^{S}\sum_{m=1}^{M} ||\mathbf{E}^{fsp}(s, m, \mathbf{u}_1^{as}, \mathbf{u}_v^{trial}) - \mathbf{E}^{meas}(s, m, \mathbf{u}_v)||^2}{\sum_{s=1}^{S}\sum_{m=1}^{M} ||\mathbf{E}^{meas}(s, m, \mathbf{u}_v)||^2} + \frac{\sum_{s=1}^{S}\sum_{m=1}^{M} ||\mathbf{H}^{fsp}(s, m, \mathbf{u}_1^{as}, \mathbf{u}_v^{trial}) - \mathbf{H}^{meas}(s, m, \mathbf{u}_v)||^2}{\sum_{s=1}^{S}\sum_{m=1}^{M} ||\mathbf{H}^{meas}(s, m, \mathbf{u}_v)||^2}. \quad (3)$$

Both these steps are much simpler than using the cost function in (1). For the first step, the forward scattering procedure is much simpler due to the lack of motion and the optimization is also simpler because the unknowns related to the velocity are not present. The second step is simpler as well, because it requires the optimization for only the velocity parameters. Since the complexity of the optimization increases much faster than linear, the two steps combined can be more efficient than doing the direct optimization of the full cost function.

For the optimization, here we adopt the differential evolution (DE) algorithm [12]. DE is a metaheuristic algorithm that starts with a random initial population of size N_p in the search space and keeps on improving the solution by introducing stochastic variations to the candidate solutions until a termination criteria is satisfied. Here the condition used for termination is that either the maximum number of iterations, N_{lim}, is reached or the cost function does not improve more than by a factor of f_{conv} in N_{conv} consecutive iterations.

III. NUMERICAL RESULTS

In this section we provide some numerical results for the reconstruction of the unknown parameters of rotating axisymmetric objects from the scattered electromagnetic fields. The simulations are performed on a Intel i7-8565U, 1.8GHz, 4 core machine with 16 GB RAM. It can be noted that for the proposed two-step algorithm, the first step involves the traditional problem of recreating the geometric and dielectric unknowns for stationary objects and is already widely studied in the literature [13]. On the other hand, the second step of the algorithm for the recreation of the rotating speeds is new and therefore is analyzed here more carefully. In Subsection III-A the proposed two-step procedure is compared to the general algorithm by solving a test case which has semi analytic solution. For this a homogeneous rotating sphere is considered. The measurement of near-field on a full circle around the scatterer is used for this and the effect of different noise levels are also studied. The same test case is used in Subsections III-B and III-C to study the accuracy of the two-step procedure with simpler sensors and with far-field data, respectively. In particular, Subsection III-B discusses the effect of having scattered field data with the measurement restricted to be on an arc in the backscattered direction and when only the amplitude data is available. Subsection III-C examines results for the far-field and the effect of uncertainty in knowing the axis of rotation of the scatterer. In Subsection III-D, the effect of changing the dielectric parameter on the accuracy of the algorithm is described. Finally in Subsection III-E a different test case is considered for which no analytic solution is available. A homogeneous rotating torus is studied for this and a numerical forward solver is exploited in the solution procedure.

A. COMPARISON OF THE TWO-STEP PROCEDURE WITH THE GENERAL ALGORITHM

We consider a simple configuration of a homogeneous sphere rotating at a uniform speed. A first order semi analytic solution is available in the literature for such a problem [1]. We analyze the performance of the general algorithm as well as that of the two-step procedure for the reconstruction of the unknown parameters.

A sphere of radius $R_s = 1$ m is considered which is rotating about the z axis at angular velocity ω_s rad/s and is illuminated by a single plane wave ($S = 1$) incident along the x axis with a frequency of $f_s = 50$ MHz. The incident electric field is polarized along the z axis. The geometry of the test case is shown in Fig. 1. The speed of rotation can be expressed in terms of the normalized quantity $\beta = \omega_s R_s / c_0$, where c_0 is the speed of light in vacuum. The results are for $\varepsilon_r = 8$ and $\beta \in \{8 \times 10^{-3}, 8 \times 10^{-4}, 8 \times 10^{-5}\}$ and are calculated at $M = 200$ points uniformly distributed on a circle on xz plane of radius $R_m = 1.5$ m from the center of the scatterer. The electric and magnetic fields thus obtained are corrupted with a Gaussian noise of specified signal to noise ratio (SNR). We consider SNR dB levels in the set $\{20, 30, 40, 50, 60\}$ added to each component of the electric and magnetic fields.

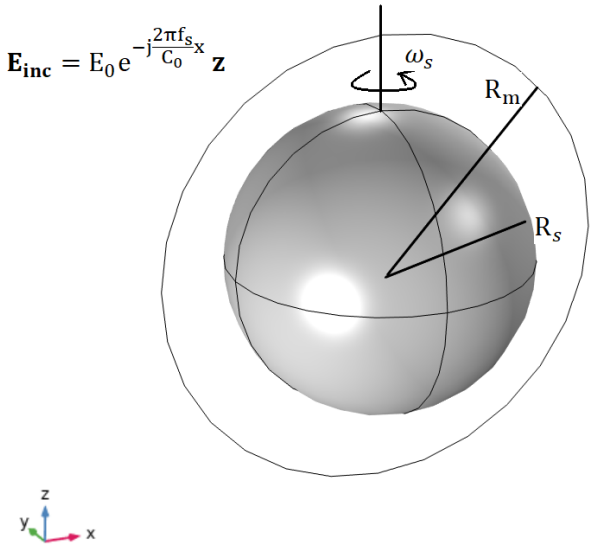

FIGURE 1. The geometry of the test case involving homogeneous spherical scatterer of radius R_s rotating about the z axis with angular velocity ω_s. It is illuminated by a plane electromagnetic wave of frequency f_s travelling along the x axis, with electric field polarized along the z axis. The measurement points are located around the sphere on a circle of radius R_m.

The inversion is carried out with the DE algorithm with a population size of $N_p = 10$. The parameters related to the termination of the algorithm are set as $N_{lim} = 100$, $f_{conv} = 0.01$ and $N_{conv} = 10$. The range over which the solutions are searched for is $\varepsilon_r \in (1, 20)$ and $\beta \in (-1, 1)$.

Table 1 summarizes the results for the case SNR = 40 dB for the three values of β indicated above. The general

Rotating speed	Algorithm	Mean relative errors		Mean number of iterations	Mean number of function evaluations	Mean minimum cost	Mean time of simulation (seconds)
		ε_r	β				
$\beta = 8 \times 10^{-3}$	General algorithm	1.39×10^{-4}	4.67×10^{-3}	40.75	427.50	3.14×10^{-4}	7398.0
	Two-step procedure	1.12×10^{-4}	2.66×10^{-3}	16.00 19.50	180.00 215.00	9.62×10^{-3} 3.04×10^{-4}	1511.1 3037.8
$\beta = 8 \times 10^{-4}$	General algorithm	1.79×10^{-4}	1.34×10^{-1}	33.50	355.00	3.16×10^{-4}	6462.8
	Two-step procedure	3.74×10^{-5}	2.54×10^{-2}	19.25 19.50	212.50 215.00	3.98×10^{-4} 3.04×10^{-4}	1332.0 3595.3
$\beta = 8 \times 10^{-5}$	General algorithm	3.05×10^{-2}	1.49×10^{2}	20.25	222.50	1.00×10^{-1}	3419.5
	Two-step procedure	1.75×10^{-4}	3.43×10^{-1}	17.50 19.25	185.00 212.50	3.16×10^{-4} 3.11×10^{-4}	1607.0 2993.3

TABLE 1. Comparison of the results obtained by the general algorithm and those of the two-step procedure for the reconstruction of the unknown parameters, ε_r and β, of rotating sphere. The data is for a SNR level of 40 dB in each component of the measured data. The sphere is of radius $R_s = 1$ m, while the illuminating field has a frequency of $f_s = 50$ MHz and a direction of propagation which is perpendicular to the axis of rotation of the sphere. The actual value of ε_r is 8. Three values of the speed β are considered and the results are averaged over four test runs.

algorithm tries to find both the unknowns together using the DE algorithm with the cost function in (1) and with $\mathbf{u} = (\varepsilon_r, \beta)$. As described in the previous section, the two-step procedure first tries to find the solution for $\mathbf{u}_1 = \varepsilon_r$ by minimizing the cost function in (2) by ignoring any rotation of the media. The approximate solution thus found in the first step is then used in the second step to solve for the value of $\mathbf{u}_2 = \beta$ by minimizing the cost function in (3).

Considering the stochastic nature of the optimization algorithm, all the results are averaged over four test runs for each configuration. As can be seen from the table, for SNR = 40 dB, both the algorithms give good results when the value of $\beta = 8 \times 10^{-3}$. The relative errors in ε_r are 0.0139 percent and 0.0112 percent for the general algorithm and the two-step procedure respectively. The corresponding relative errors in β are 0.467 percent and 0.266 percent. However, the two-step procedure is able to find the solution in 1 hour and 15 minutes whereas the general algorithm took 2 hours and 3 minutes to find the solution. The performance of the two-step procedure improves relative to the general procedure when the rotating speeds are lower. For $\beta = 8 \times 10^{-4}$, the two-step procedure obtains the solutions for ε_r and β with relative errors of 0.00374 percent and 2.54 percent respectively. The corresponding relative errors in the solution obtained from the general algorithm are 0.0179 percent and 13.4 percent. Finally when $\beta = 8 \times 10^{-5}$, the general algorithm give completely unreliable result for β while the two-step procedure gives a value with 34.3 percent relative error.

In conclusion, the two-step procedure provides more accurate solutions than the general algorithm as the rotating speed gets lower. The time of simulation is much lower for the two-step procedure than the general algorithm. The solutions are reliable for lower values of speed as long as the noise level is not too high. It can be noted that although the two-step procedure is proposed assuming that the speeds are not too high, the numerical results show that it is applicable even for the highest of the velocity values that can be of practical relevance.

To get an indication on how larger values of rotating speed can affect the accuracy of the two-step algorithm, the error values from both the algorithms are provided in Fig. 2 for β values in the set $\{4 \times 10^{-3}, 8 \times 10^{-3}, 1.6 \times 10^{-2}, 3.2 \times 10^{-2}, 6.4 \times 10^{-2}, 1.28 \times 10^{-1}\}$. The results indicate that, for the homogeneous medium considered ($\varepsilon_r = 8$), the two-step algorithm performs better than the general algorithm for values of β that are less than around 2.75×10^{-2}. Although the exact values can change with the dielectric medium, the results confirm that the two-step algorithm provides accurate results for all practical speeds that can be of interest.

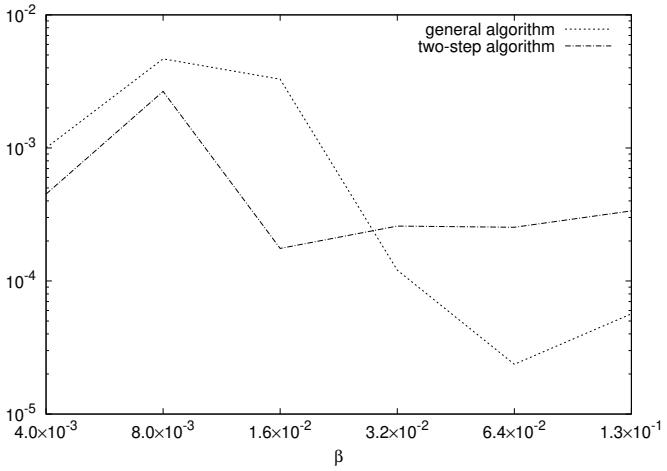

FIGURE 2. The mean relative error in the reconstructed value of β vs the value of β for the rotating sphere. The result obtained from the two-step algorithm is compared with that obtained using the general algorithm. The measured fields are corrupted with SNR level of 40 dB.

To better understand how the results of the two-step procedure are affected by the noise in the scattered field data we give the effect of SNR values on the error in the reconstructed speed obtained using the two-step procedure. In Fig. 3 the mean relative error in the reconstructed value of β is plotted against the SNR levels in dB. The plots for three rotating speeds, $\beta \in \{8 \times 10^{-3}, 8 \times 10^{-4}, 8 \times 10^{-5}\}$, are shown. For $\beta = 8 \times 10^{-3}$, the relative error is just 0.032 percent for SNR = 60 dB and it increases to 8.2 percent when SNR = 20 dB. When $\beta = 8 \times 10^{-4}$, the average relative error values are 0.35 percent for SNR = 60 dB and 27 percent for SNR = 20 dB. Finally, for $\beta = 8 \times 10^{-5}$, the average relative errors are 4.47 percent for SNR = 60 dB and 493.6 percent for SNR = 20dB. It can be noted that for small values of β the effects of motion on the electromagnetic field are small and the noise can easily affect the field more than motion. In these cases accurate measurements of the field are necessary. It is interesting to point out, however, that if this is done good results can be achieved.

B. PERFORMANCE OF TWO-STEP PROCEDURE WITH SIMPLER SENSORS

In the previous subsection we examined the performance of the reconstruction algorithm when the measurement of the complex fields was available on the full circle outside the scatterer. Now we examine the performance of the two-step

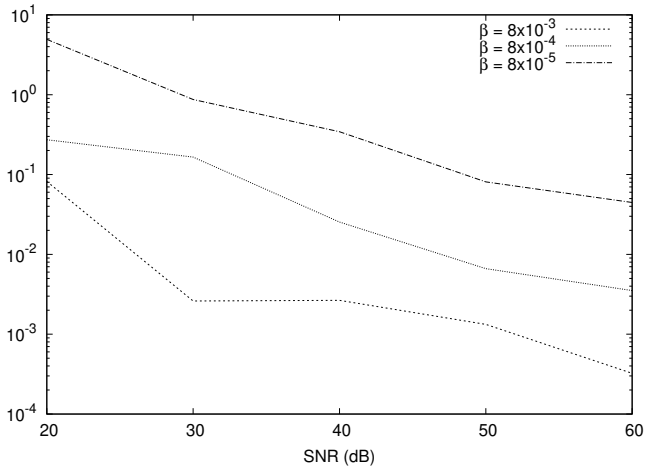

FIGURE 3. The mean relative error in the reconstructed value of β vs the SNR levels in dB for the rotating sphere. The results are shown for three different values of β.

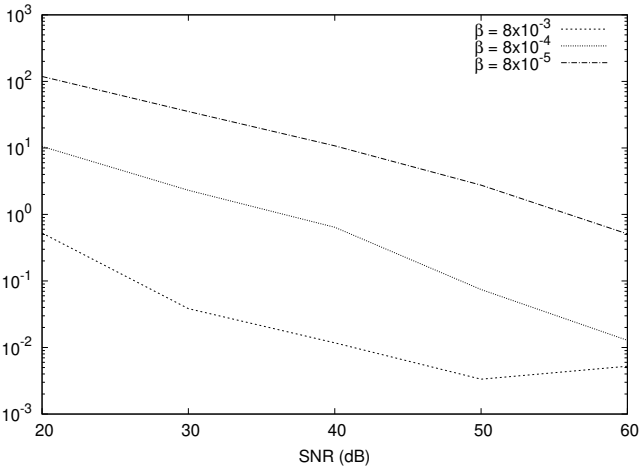

FIGURE 5. The mean relative error in the reconstructed absolute value of β vs the SNR levels in dB for the rotating sphere using amplitude only data in the backscattered direction. The results are shown for three different values of β.

algorithm under limitations introduced by the sensors. First we study the effect of restricting the measurement points to only a small portion along the backscattering direction. After that we also investigate the effect of having only the amplitude data for the electromagnetic fields which can allow us to use much simpler sensors.

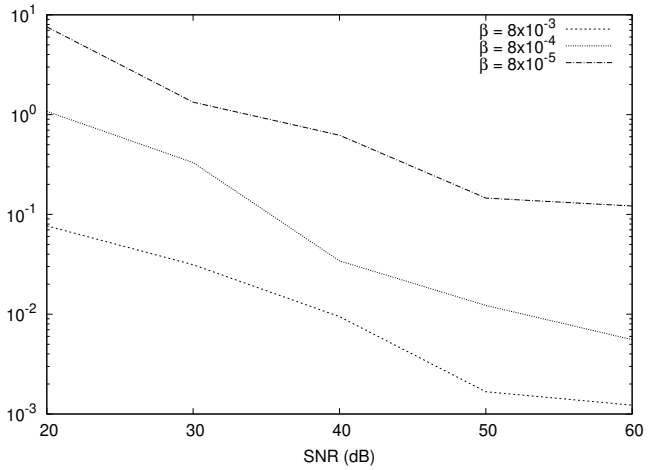

FIGURE 4. The mean relative error in the reconstructed value of β vs the SNR levels in dB for the rotating sphere using data in the backscattered direction. The results are shown for three different values of β.

The results obtained by considering only the measurement points along the backscattered direction are provided in Fig. 4. For this we use only the portion of measurement data that belongs to an arc subtending an angle of 90 degrees along the backscattering direction. So we considered 50 measurement points on an arc on xz plane of radius 1.5 m from the center of the scatterer. It is observed that the reconstruction algorithm still works well with such a restriction. For example for $\beta = 8 \times 10^{-4}$ and with SNR = 60 dB, the relative error in the reconstructed value of β is 0.55 percent as compared to 0.35 percent obtained previously using the data on the full circle. For $\beta = 8 \times 10^{-4}$ and SNR = 40 dB, the corresponding values are 3.4 percent and 2.5 percent. With $\beta = 8 \times 10^{-4}$ and SNR = 20 dB the errors become 108.1 percent using the data along backscattered direction as opposed to 27.3 percent with the data on the full circle.

Next we examine the effect of using sensors that can measure only the amplitude of the electromagnetic fields. For this case we have to modify the cost functions involved so that only differences in the magnitudes of each component of the fields are considered. The measurement points used for the reconstruction are the same as those in the previous step involving only backscattered fields. In this case it is not possible to distinguish between the clockwise and anti-clockwise rotations and therefore we have to consider only the absolute value of the reconstructed β. The results are provided in Fig. 5. As expected, the accuracy is not as good as that obtained with both amplitude and phase information. For example, with $\beta = 8 \times 10^{-4}$ and with SNR = 40 dB, the error in the reconstructed speed is 64.1 percent as opposed to 3.4 percent obtained using both amplitude and phase measurements. However, with less noisy data the accuracy is acceptable as in the case with $\beta = 8 \times 10^{-4}$ and with SNR = 60 dB, where we get an error in the reconstructed speed of 1.28 percent. Similar comparisons can be made for the case of $\beta = 8 \times 10^{-3}$ and $\beta = 8 \times 10^{-5}$ shown in the figures and the results are good when the speed is not very small and the SNR is good enough.

Therefore in conclusion, we still get good solutions for the rotating speeds when the measurement is restricted to the backscattering direction. The results are degraded when only amplitude data are available but the errors are still small provided that the noise does not overwhelm the effects of motion.

C. RECONSTRUCTION OF THE SPEED OF ROTATION FROM FAR-FIELD DATA

So far, we concentrated on the performance of the reconstruction algorithm using the total field data in the near-field region. Next, let us analyze the performance of the algorithm with the scattered electromagnetic field in the far-field region. For this we consider the measurement arc on xz plane in the backscattered direction of radius 1.5×10^3 m from the center of the scatterer. The results are plotted in Fig. 6.

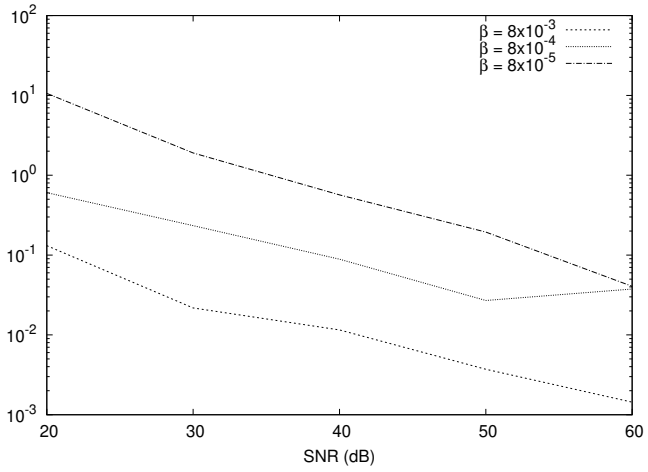

FIGURE 6. The mean relative error in the reconstructed value of β vs the SNR levels in dB for the rotating sphere using far-field data in the backscattered direction. The results are shown for three different values of β.

The algorithm performs well for $\beta = 8 \times 10^{-3}$ and the error for SNR values greater than or equal to 30 dB is less than 2.2 percent and is 13.1 percent for SNR of 20 dB. However, for $\beta = 8 \times 10^{-4}$, the error in the reconstructed value of β is 3.7 percent for SNR of 60 dB and is around 9 percent for 40 dB and rises to 23 percent for 30 dB SNR. Finally, for $\beta = 8 \times 10^{-5}$, the reconstruction algorithm performs very poorly for the considered values of SNR. The error for 60 dB SNR in the data is 4 percent while for 50 dB the error is 19.3 percent and rises to unacceptable levels as the noise increases.

Let us also examine the effect of error in the knowledge of the axis of rotation of the scatterer. For this we may generate the measurement data using the forward model on an arc whose plane is rotated by an angle α from the xz plane while still using the old set of points for the reconstruction algorithm. The results with such an approach is shown in Fig. 7 for $\alpha = 10°$. For $\beta = 8 \times 10^3$, the algorithm is able to find the value of the rotating speed with an error of less than 1.6 percent for SNR values greater than or equal to 30 dB. The error for $\beta = 8 \times 10^{-4}$ is 1.3 percent for SNR of 60 dB, 15.1 percent for SNR of 40 dB and 22.8 percent for SNR of 30 dB. Finally, for $\beta = 8 \times 10^{-5}$, the results for the considered values of SNR are unreliable with a 36 percent error even for SNR of 60 dB, which rises to a 102 percent error for SNR of 40 dB.

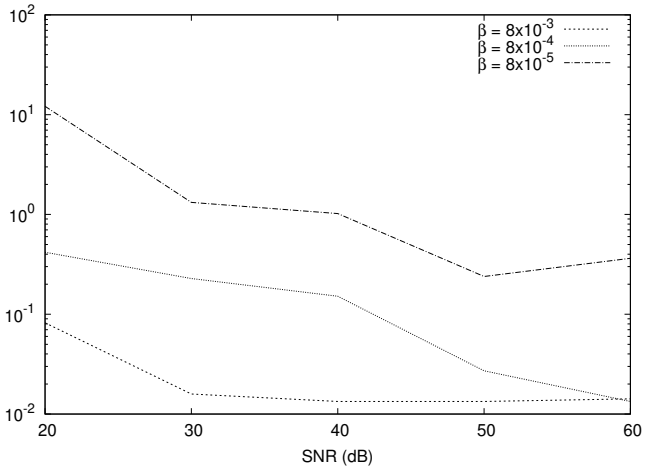

FIGURE 7. The mean relative error in the reconstructed value of β vs the SNR levels in dB for the rotating sphere using far-field data in the backscattered direction and $\alpha = 10°$. The results are shown for three different values of β.

D. THE EFFECT OF DIFFERENT DIELECTRIC MEDIA

Let us also examine the effect of changing the dielectric parameter, ε_r, on the accuracy of the reconstructed speed. The result for a rotating speed of $\beta = 8 \times 10^{-4}$ is presented in Fig. 8. The measurements are considered at $M = 200$ points on a circle of radius $R_m = 1.5$ m. The permittivity values considered are $\varepsilon_r \in \{4, 8, 12, 16, 20\}$, and the results are shown for three noise levels, SNR $\in \{30, 40, 50\}$ (dB). The reconstruction becomes more difficult if the scattering is weak and therefore we can in general expect a larger error for smaller values of ε_r. This trend can be confirmed from the obtained results. For instance, with SNR = 40 dB, the relative error is 25.7 percent for $\varepsilon_r = 4$ while it reduces to 0.37 percent for $\varepsilon_r = 20$. Similarly the error goes from 140 percent to 1.5 percent for SNR = 30 dB and from 2.99 percent to 0.069 percent for SNR = 50 dB, as ε_r increases from 4 to 20.

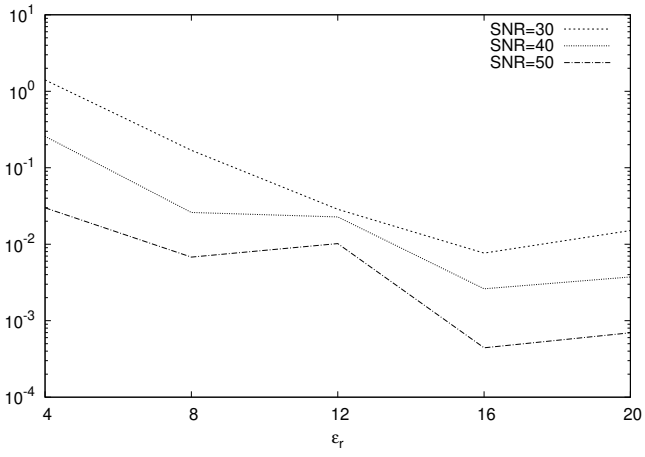

FIGURE 8. The mean relative error in the reconstructed value of β vs ε_r for the rotating sphere with $\beta = 8 \times 10^{-4}$ and the measurements are considered at $M = 200$ points on a circle of $R_m = 1.5$ m. The results are shown for three different values of SNR.

E. RECONSTRUCTION OF THE SPEED OF ROTATING TORUS

All the previous results were obtained for rotating sphere which admits a semi analytic solution for the forward problem. Now we apply the algorithm to rotating homogeneous torus for which analytic solutions are not available; a numerical forward solver has to be exploited instead. The direct solution for the fields is obtained using a finite element method [14], [8]. The solver is implemented using a model in the commercial simulator COMSOL Multiphysics (COMSOL, Burlington, MA). The axis of symmetry of the torus is taken as the z axis about which the torus rotates with an angular velocity of ω_s. The major radius, R_{tor}, and the minor radius, r_{tor}, of the torus [8] are taken as respectively 0.75 m and 0.25 m. The geometry of the test case is shown Fig. 9. We may express the speed of rotation using the normalized quantity $\beta = \frac{\omega_s(R_{tor}+r_{tor})}{c_0}$. The scattering medium at rest is characterized by $\varepsilon_r = 8$ and $\mu_r = 1$. It is illuminated by a plane wave incident along the x axis, polarized along z axis and with a frequency $f_s = 150$ MHz.

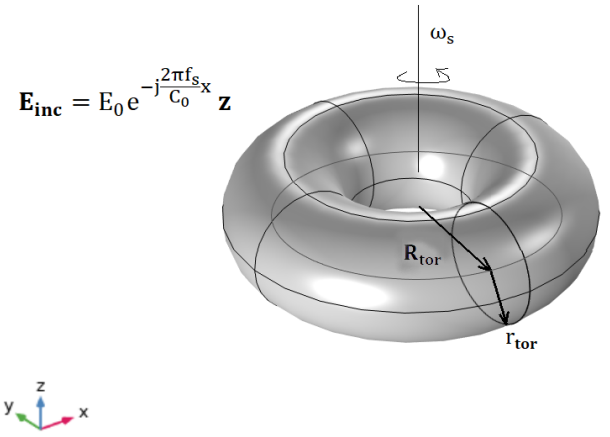

FIGURE 9. The geometry of the test case involving homogeneous toroidal scatterer of major radius R_{tor} and minor radius r_{tor} rotating about the z axis with angular velocity ω_s. It is illuminated by a plane electromagnetic wave of frequency f_s travelling along the x axis, with electric field polarized along the z axis.

The numerical domain is set to $R_d = 4$ m and the measurement data are taken at $M = 200$ uniformly placed points on a circle in xz plane of radius $R_m = 1.5$ m. The variational formulation is implemented in the mathematics module of the COMSOL Multiphysics using a second order edge element formulation. A tetrahedral meshing is done with 241181 elements, 41605 nodes and 9438 boundary elements. The algebraic solver used is GMRES with a tolerance of 10^{-4} and with geometric multigrid preconditioner. The reconstruction algorithm searches for the optimal value of β in the range $(0, 10^{-2})$ and the parameters of the DE optimizer are the same as before ($N_p = 10$, $N_{lim} = 100$, $f_{conv} = 0.01$, $N_{conv} = 10$). The measured data is corrupted with noise as before with SNR levels varying from 20 dB to 60 dB. Compared to the analytical solutions, the numerical solvers produce additional noise, due to discretization errors and the tolerance in algebraic solver, which could affect the performance of the inverse algorithm.

The results are shown in Fig. 10 for values of $\beta \in \{8 \times 10^{-3}, 8 \times 10^{-4}, 8 \times 10^{-5}\}$. For $\beta = 8 \times 10^{-3}$, the relative error in the solution is less than 1.6 percent when SNR in the measured data is greater than or equal to 30 dB. In the case of $\beta = 8 \times 10^{-4}$, the relative errors are 2.14 percent for 50 dB SNR, 13.9 percent for 40 dB SNR and 21.6 percent for 30 dB SNR. When $\beta = 8 \times 10^{-5}$, the relative errors are very high. It is 16.7 percent for 60 dB SNR, 29.9 percent for 50 dB SNR and more than 100 percent when SNR is greater than or equal to 40 dB. As mentioned before, the additional noise in the numerical solver is a reason for the worse performance of the reconstruction algorithm compared to the case with semi analytic forward solver. In particular, for small values of the rotating speed, we need not only to perform very accurate measurements of the fields but also to reduce numerical errors in order to get reliable results.

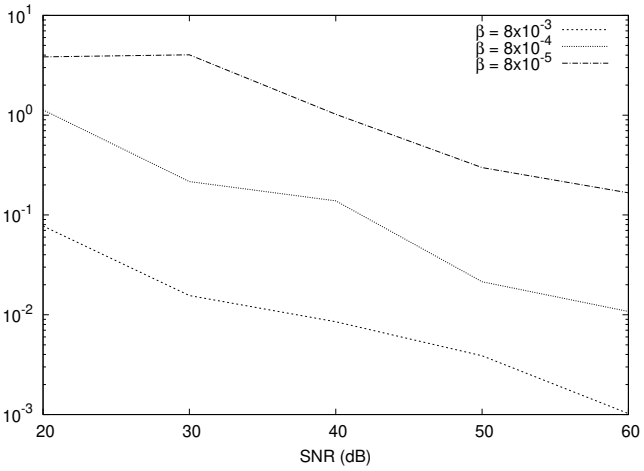

FIGURE 10. The mean relative error in the reconstructed value of β vs the SNR levels in dB for the rotating torus with measurement data on a circle of radius $R_m = 1.5$ m on the xz plane. The results are shown for three different values of β.

IV. CONCLUSION

In this paper, the electromagnetic inverse problem involving rotating axisymmetric objects was studied for the first time. We investigated the reconstruction of the rotating speeds of axisymmetric objects from the scattered field data. A two-step algorithm was proposed for the inversion when the speeds are known to be not too large. In the first step, forward solver is employed assuming zero rotating speed and the geometric and dielectric data are reconstructed by minimizing the cost function. In the second step, the values from the first step are used to determine the rotating speed. By defining a test case involving rotating homogeneous sphere, the two- step procedure is compared with the straightforward inversion procedure which solves for all the unknowns together. It was established that the two-step procedure is much faster and also more accurate if the rotating speeds

assume values of practical interest. The performance of the algorithm was tested with different types of noisy data: near-field data, far-field data and amplitude only data were used as inputs to the two-step procedure to obtain the rotating speeds. The results show that for relatively small speed values the two-step procedure can recover the velocity of rotation in a reliable way provided that the noise does not overwhelm the effects of the rotation on the field. In addition to rotating sphere, the algorithm was also applied to a rotating torus to demonstrate the generality of the results. This article studied only the test cases with homogeneous velocity profiles to give the first results on the efficiency and accuracy of the two-step procedure. However, the proposed algorithm is general and can be applied to more complex velocity profiles.

REFERENCES

[1] D. De Zutter, "Scattering by a rotating dielectric sphere," *IEEE Transactions on Antennas and Propagation*, vol. 28, no. 5, pp. 643–651, September 1980.
[2] J. G. Van Bladel, *Electromagnetic Fields*, 2nd ed. Piscataway, NJ, USA: IEEE Press, 2007.
[3] C. Yeh, "Reflection and transmission of electromagnetic waves by a moving plasma medium," *Journal of Applied Physics*, vol. 37, no. 8, pp. 3079–3082, July 1966.
[4] Y. Yan, "Mass flow measurement of bulk solids in pneumatic pipelines," *Measurement Science and Technology*, vol. 7, no. 12, p. 1687, 1996.
[5] M. Li, Y. Hu, R. Chen, and G. Vecchi, "Electromagnetic modeling of moving mixed conductive and dielectric bors with an effective domain decomposition method," *IEEE Transactions on Antennas and Propagation*, vol. 68, no. 12, pp. 7978–7985, 2020.
[6] D. K. Cheng and J.-A. Kong, "Covariant descriptions of bianisotropic media," *Proceedings of the IEEE*, vol. 56, no. 3, pp. 248–251, March 1968.
[7] M. Pastorino and M. Raffetto, "Scattering of electromagnetic waves from a multilayer elliptic cylinder moving in the axial direction," *IEEE Transactions on Antennas and Propagation*, vol. 61, no. 9, pp. 4741–4753, September 2013.
[8] P. Kalarickel Ramakrishnan and M. Raffetto, "Well posedness and finite element approximability of three-dimensional time-harmonic electromagnetic problems involving rotating axisymmetric objects," *Symmetry*, vol. 12, no. 2, p. 218, 2020.
[9] M. Pastorino, M. Raffetto, and A. Randazzo, "Electromagnetic inverse scattering of axially moving cylindrical targets," *IEEE Transactions on Geoscience and Remote Sensing*, vol. 53, no. 3, pp. 1452–1462, March 2015.
[10] M. Brignone, G. L. Gragnani, M. Pastorino, M. Raffetto, and A. Randazzo, "Noise limitations on the recovery of average values of velocity profiles in pipelines by simple imaging systems," *IEEE Geoscience and Remote Sensing Letters*, vol. 13, no. 9, pp. 1340–1344, 2016.
[11] P. Kalarickel Ramakrishnan and M. Raffetto, "Three-dimensional time-harmonic electromagnetic scattering problems from bianisotropic materials and metamaterials: Reference solutions provided by converging finite element approximations," *Electronics*, vol. 9, no. 7, p. 1065, 2020.
[12] R. Storn and K. Price, "Differential evolution–a simple and efficient heuristic for global optimization over continuous spaces," *Journal of global optimization*, vol. 11, no. 4, pp. 341–359, 1997.
[13] M. Pastorino, *Microwave imaging*. John Wiley & Sons, 2010, vol. 208.
[14] J. Jin, *The finite element method in electromagnetics*. New York: John Wiley & Sons, 1993.